

Update on patterns of pulmonary infection in immunocompetent patients

Actualización en los patrones de infecciones pulmonares en pacientes inmunocompetentes

José David Brito Araújo[1]
Felipe Aluja Jaramillo[2]
Alberto Latorre Pinto[1]
Liliana Arias Álvarez[3]
Helí Rueda Chaparro[4]
Julia Andrea Rodríguez[4]
https://doi.org/10.53903/01212095.354

Key words (MeSH)

Pneumonia
Bronchopneumonia
Lung
Tomography, X-Ray computed
Radiography, thoracic

Palabras clave (DeCS)

Neumonía
Bronconeumonía
Pulmón
Tomografía computarizada por rayos X
Radiografía torácica

Summary

Many pathogens can infect the lungs and cause pneumonia in immunocompetent patients. These agents include bacteria, but also viruses, fungi and parasites. Recognising the radiological patterns on chest X-rays and CT scans is crucial to identifying the causative pathogens and possible complications, and thus improving the clinical management strategy. An accurate approach facilitates the administration of effective therapies, which can significantly improve the patient's prognosis.

Resumen

Múltiples agentes patógenos pueden infectar el pulmón y desencadenar neumonía en pacientes inmunocompetentes. Estos agentes incluyen principalmente bacterias, pero también virus, hongos y parásitos. El reconocimiento de los patrones radiológicos en radiografías y tomografías computarizadas del tórax es crucial para identificar los patógenos causantes, así como las posibles complicaciones y optimizar la estrategia clínica del tratamiento. Una aproximación precisa facilita la administración de terapias efectivas, lo que puede mejorar significativamente el pronóstico del paciente.

[1]Physician, Radiology Resident, Hospital Universitario San Ignacio, Pontificia Universidad Javeriana. Bogotá, Colombia.

[2]Radiologist, Master's degree in Education for Health Professionals, Assistant Professor, Department of Radiology, Hospital Universitario San Ignacio, Pontificia Universidad Javeriana, and Professor in the Specialization and Master's Program in Education for Health Professionals, Pontificia Universidad Javeriana–Universidad del Rosario Partnership. Bogotá, Colombia. ORCID: https://orcid.org/0000-0002-3093-2509.

[3]Physician, specialist in Radiology and Diagnostic Imaging, Hospital Universitario San Ignacio. Bogotá, Colombia.

[4]Physician, specialist in Radiology and Diagnostic Imaging. Bogotá, Colombia.

Introduction

Pneumonia is the leading cause of death from infectious diseases worldwide and the sixth leading cause of overall mortality (1). It is defined as inflammation of the air spaces and/or interstitium, associated with symptoms of infection and an acute infiltrate on a chest X-ray (1, 2). Risk factors include adults, children under 5 years of age, immunocompromised patients, and comorbidities (COPD, heart failure, chronic kidney disease, diabetes mellitus, etc.).

Clinical classification of pneumonia

Community-acquired pneumonia is pneumonia acquired outside the hospital, in the community setting (2). Hospital-acquired pneumonia is pneumonia acquired more than 48 hours after admission, and hospitalization is always required for it to be classified as such (this does not include long-term care facilities, rehabilitation centers, or other healthcare settings) (2). Ventilator-associated pneumonia is pneumonia acquired more than 48 hours after endotracheal intubation (2, 3).

Physiopathology

There are four main mechanisms involved in lung defense: the cough reflex, mucociliary clearance, IgA-containing mucus production, and humoral immunity (as measured by complement activity) and cell-mediated immunity (2). Infection occurs when one of these mechanisms is compromised or when the infectious load is very high (2). For pneumonia to develop, the pathogen must reach the alveoli, and the host's defenses must be overcome by the microorganism's virulence. Routes of entry include inoculation through the tracheobronchial tree via droplets or aerosols, aspiration of oropharyngeal secretions, or by direct contact.

Diagnostic imaging evaluation

The first-line imaging modality is chest X-ray; however, determining the etiology based solely on chest X-ray is unreliable (3). Chest X-ray is used in immuno-

competent patients with acute respiratory illness, whether or not they have a positive physical examination, normal or abnormal vital signs, and with or without risk factors (4). In immunocompetent patients with acute respiratory illness and a positive physical examination, abnormal vital signs, and risk factors, but with a normal X-ray, a non-contrast chest CT scan is preferred (4). In immunocompetent patients with pneumonia complicated by pleural effusion or abscess, a contrast-enhanced chest CT scan is preferred (4). A CT scan is also preferred in cases of unexpected clinical progression and suspicion of an underlying lesion (3, 4). Ultrasound is preferred for evaluating pleural effusion or empyema and for guiding aspiration or drainage.

Clinical findings and radiological patterns

Semiological findings in pulmonary infections include consolidations, "ground-glass" opacities, bronchiectasis obstructed by secretions, nodules, patchy opacities, and cavitations (Figure 1).

Radiological patterns include:

- **Lobar pattern:** the most common presentation of community-acquired pneumonia (CAP), with inflammatory exudate in distal air spaces adjacent to the visceral pleura, spreading through Lambert's collateral air shunts and Kohn's pores, involving a lobe completely or partially, with homogeneous consolidation delimited by the fissure, with or without an air bronchogram (5–9) (Figure 2).
- **Bronchopneumonic pattern:** microorganisms settle on the bronchial epithelium, causing acute bronchial inflammation, epithelial ulcerations, and the formation of peribronchiolar exudate, which extends to the peripheral airways (6–9). The involvement forms nodules that tend to coalesce and generate areas of consolidation in predominantly peripheral patches (5) (Figure 3). This is the most common manifestation in S. aureus, H. influenzae, and P. aeruginosa (6–8).
- **Interstitial pattern:** caused by an inflammatory cellular infiltrate in the alveolar septa and the distal peribronchovascular interstitium, secondary to epithelial damage, with thickening of the peribronchial zone and the interlobular septa, as well as inflammation extending to a lesser degree into the airspace, with "ground-glass opacity" and centrilobular nodules (6, 7, 9) (Figure 4).

Etiological Classification of Pneumonia

Pneumonia is also classified according to the causative agent, which may be bacterial, viral, fungal, or parasitic. The characteristics of each agent are described below.

- Bacterial agents
  - ***Streptococcus pneumoniae:*** This is the most common cause of CAP and the prototypical pathogen responsible for lobar or multifocal consolidation (3, 8) (Figure 2). The most significant risk factors include extreme ages and underlying pulmonary and cardiac diseases (6). Lymphadenopathy and pleural effusion are seen in 50% of patients; cavitation is uncommon, and anaerobic organisms should be considered when it occurs (8). The infection may be spherical, especially in children, due to the absence of interalveolar communications (3, 6) (Figure 5).
  - ***Staphylococcus aureus:*** This is a common cause of healthcare-associated pneumonia (HAP), particularly in intensive care units (ICUs) (3, 6). It is more common in patients who use intravenous drugs or have indwelling intravenous catheters (3, 7). It can be a complication of a viral infection (7). In most cases, it presents with a pattern of segmental bronchopneumonia predominantly in the lower lobes, which may be unilateral or bilateral (3, 7) (Figure 3). Abscess formation occurs in 15–30% of cases, and pleural effusion in 30–50%, with empyema in half of the cases (8). Pneumoceles are more common in children and can cause pneumothorax (7, 8). Hematogenous spread of the infection results in a presentation known as septic embolism, characterized by multiple peripheral nodular masses with or without cavitation (7) (Figure 6).
  - ***Haemophilus influenzae:*** a Gram-negative bacillus that, in some populations, is the second most common cause of pneumonia (1). It is common in patients with COPD, in whom it colonizes the upper airways, as well as in individuals with endobronchial neoplasms, smoking, and alcoholism (3). It presents with a bronchopneumonic pattern, thickening of the bronchial walls, centrilobular nodules, "ground-glass opacity," and consolidations (6) (Figure 7).
  - ***Klebsiella pneumoniae:*** typically occurs in older adults with chronic lung disease or in alcoholics (6). It presents as a homogeneous, non-segmental consolidation that rapidly spreads to become lobar pneumonia (predominantly in the right upper lobe) (7). Cavitation may occur in 30–50% of cases, which distinguishes it from pneumonia caused by pneumococcus (7) (Figure 8). Pleural effusion and empyema are often found. Lobar expansion with bulging of the fissures may be observed (more common before the antibiotic era) (7, 9, 10).
  - **Anaerobic bacteria:** are the result of aspiration of infected oral contents; many patients have evident periodontal disease (11–14). Most infections are polymicrobial (15). Risk factors include altered consciousness, dysphagia, and alcoholism (7). Consolidation with or without cavitation is observed, predominantly in the posterior segment of the maxilla and in the upper part of the mandible; this manifests when lying down and in the basal position in standing patients, with a predominance on the right side (Figure 9). Hilar and mediastinal lymphadenopathy may accompany the abscess and may resemble carcinoma (7). One-third of patients present with empyema (16).

- ***Mycobacterium tuberculosis:*** Tuberculosis remains a global problem, with a prevalence of 32% (17, 18). The most significant risk factors include HIV, diabetes, gastrectomy, homelessness, living in nursing homes, being an immigrant, and exposure to silica (5, 7). It is transmitted through the respiratory tract via droplets and causes nonspecific focal pneumonia (Ghon's focus) (7). An initial infection known as primary tuberculosis occurs: the bacteria are ingested by macrophages and spread to the lymph nodes (5). Its presentation depends on the immune response (5). 30% of people will develop the primary infection; of these, the host is asymptomatic in 95% of cases, and only 5% will experience early progression. Subsequently, of the 95% who were asymptomatic, only 5% will experience reactivation. Containment is represented by calcified nodules in the parenchyma and hilar lymph nodes (Rathke's complex).

  Primary tuberculosis is more common in young children and immunocompromised individuals (7, 19). Initially, it spreads to local lymph nodes, and lymphadenopathy is the most common manifestation in children with or without pneumonia (3) (Figure 10). Hilar lymphadenopathy is usually unilateral, but in some patients it may be bilateral, or mediastinal lymphadenopathy may occur in isolation (7, 20). It presents as lobar pneumonia, commonly in the lower lobes and on the right side (without predilection), with centrilobular nodules of atypical distribution (different from those in the upper lobes) (5). Cavitation is uncommon, and pleural effusion is frequent (7).

  Post-primary tuberculosis can occur at any time after the initial infection (5). It presents as irregular subsegmental consolidations in the posterior segments of the upper lobes and the upper segments of the lower lobes (7, 21). Lymphadenopathy is uncommon, and cavitation is common, particularly in the upper lobes (3, 5, 7) (Figure 11). Endobronchial spread may occur with or without cavitary disease and is similar to that seen in primary tuberculosis, resulting in a "branching tree" pattern (5, 22, 23).

- **Nontuberculous mycobacteria:** account for 1–3% of mycobacterial infections (3). Risk factors include an underlying debilitating disease, immunosuppression, chronic airflow obstruction, previous pulmonary tuberculosis, or silicosis (3, 24). There are different types of mycobacteria that are common in the natural environment (7, 25, 26). The mycobacteria most frequently capable of causing pulmonary infection are: M. avium-intracellulare, M. kansasii, M. abscessus, and M. xenopi (27–29). The classic form produces a presentation similar to that of reactivated tuberculosis, with consolidations, cavitations, or centrilobular nodules in the upper lobes (5). The nonclassic form occurs in older women without prior lung disease. It is noncavitary and manifests as cylindrical bronchiectasis associated with multiple focal pulmonary nodules, with a higher prevalence in the lingula and middle lobe (5) (Figure 12).

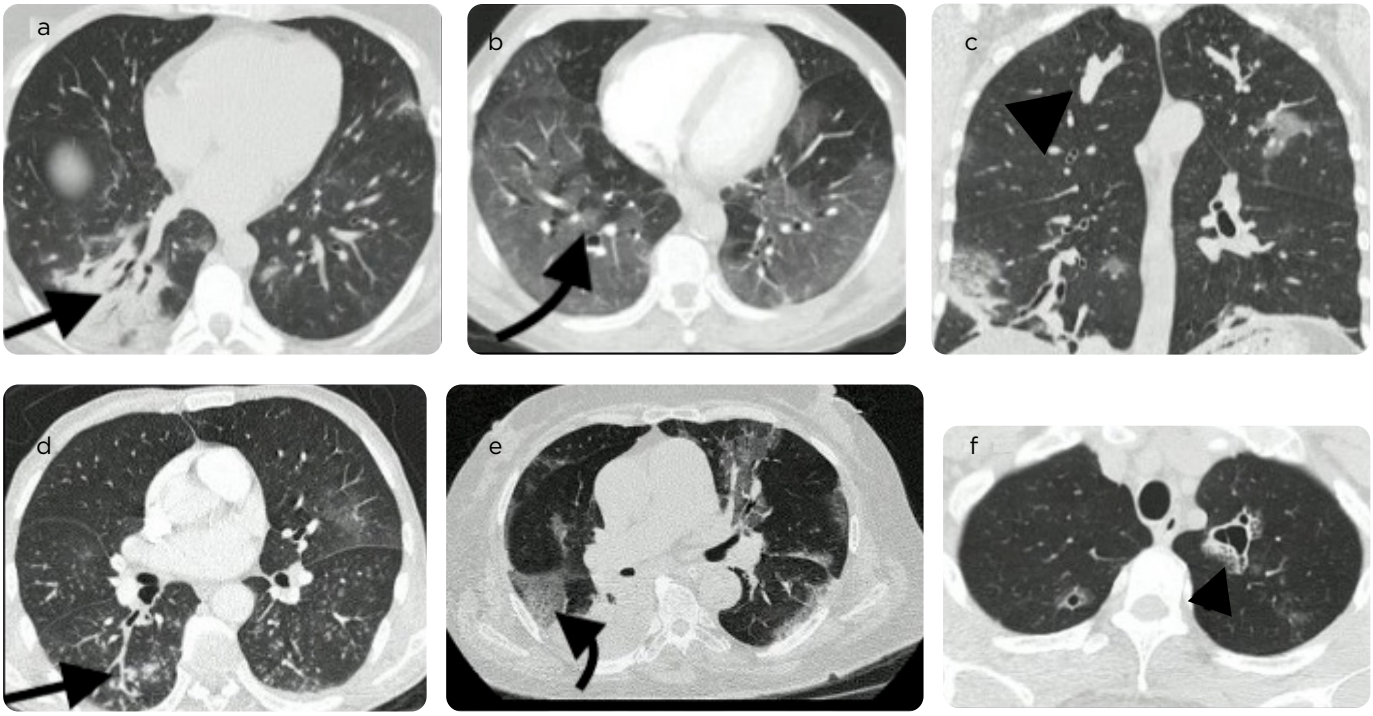


Figure 1. a, b, d, e, and f) Chest CT scans in lung window mode (axial sections) and c) Chest CT scan in lung window mode (coronal reconstruction). a) Lobar consolidation in a patient with community-acquired pneumonia (arrow). b) "Ground-glass opacity" in a patient with COVID-19 infection (curved arrow). c) Bronchiectasis obstructed by secretions in a patient with allergic bronchopulmonary aspergillosis (ABPA) (arrowhead). d) Centrilobular nodules in a patient with bronchopneumonia (arrow). e) Cobblestone pattern in a patient with viral pneumonia (curved arrow) and f) Cavities in both upper lobes (arrowhead) in a patient with Mycobacterium tuberculosis infection.

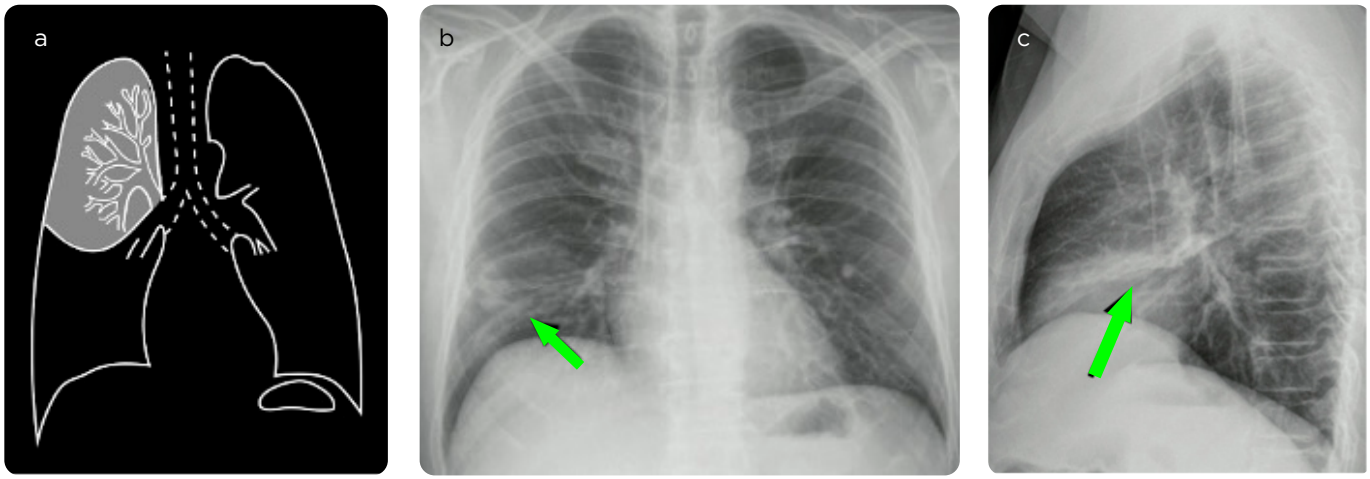


Figure 2. a) Schematic diagram. b and c) Chest X-ray in PA and lateral views. a) Pattern of lobar pneumonia, with homogeneous consolidation delimited by the fissure and air bronchogram. b and c) More or less well-defined homogeneous consolidation (black arrows), without signs of volume loss and with an air bronchogram in the middle lobe, in a 40-year-old woman with S. pneumoniae pneumonia.

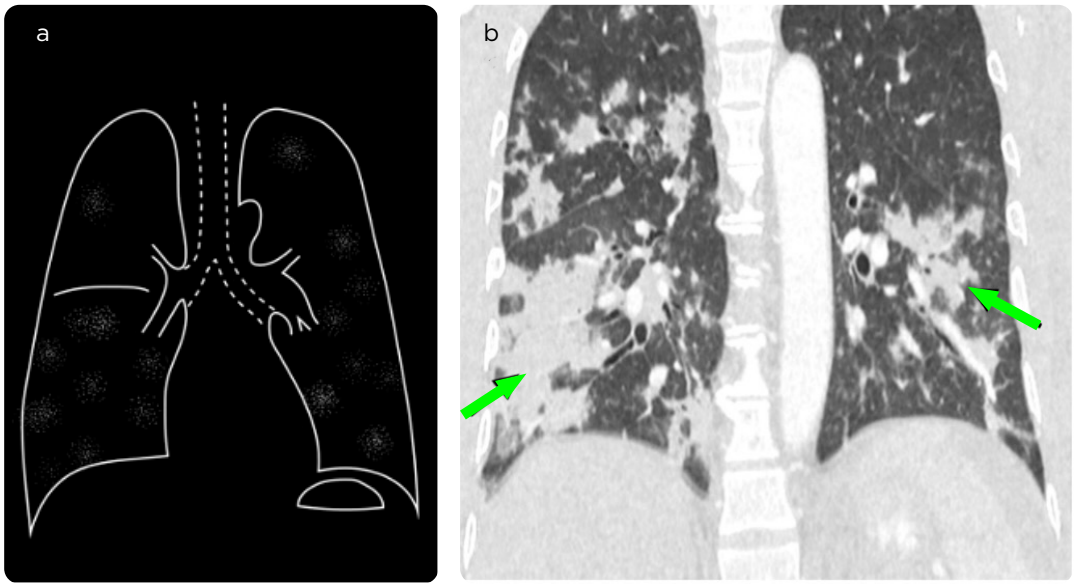


Figure 3. a) Schematic diagram b) Chest CT scan in lung window, coronal reconstruction. a) Ill-defined centrilobular nodules, airspace nodules, and multifocal areas of lobular consolidation. b) Multiple bilateral lobular consolidations and some centrilobular nodules predominantly in the lower lobes (black arrows), in a patient with S. aureus infection.

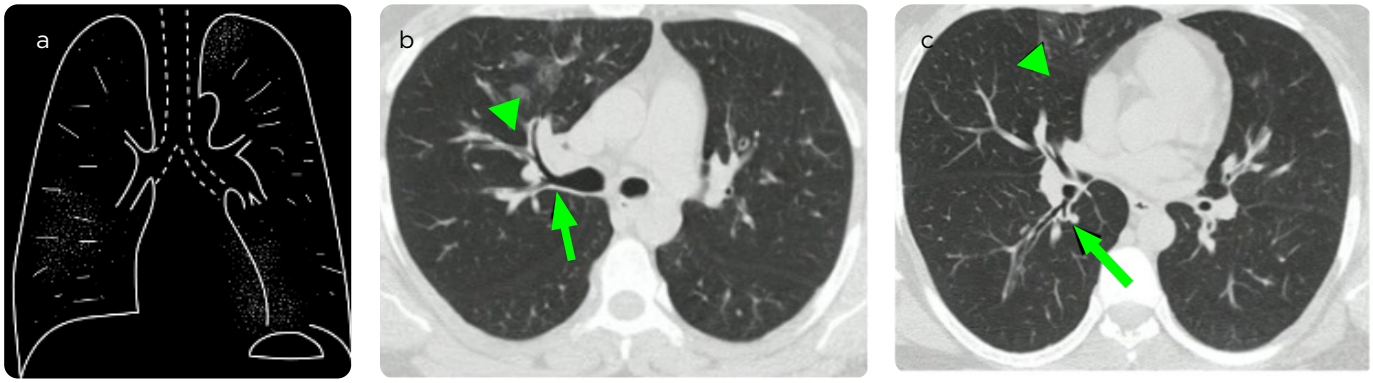


Figure 4. a) Schematic. b and c) Chest CT scan in lung window with axial reconstructions. a) Interstitial pneumonia (thickening of the terminal bronchi, reticular opacities, and "ground-glass" opacities). b and c) Thickening of the central bronchial walls (arrows) and areas of "ground-glass" opacities in the right upper lobe (arrowheads).

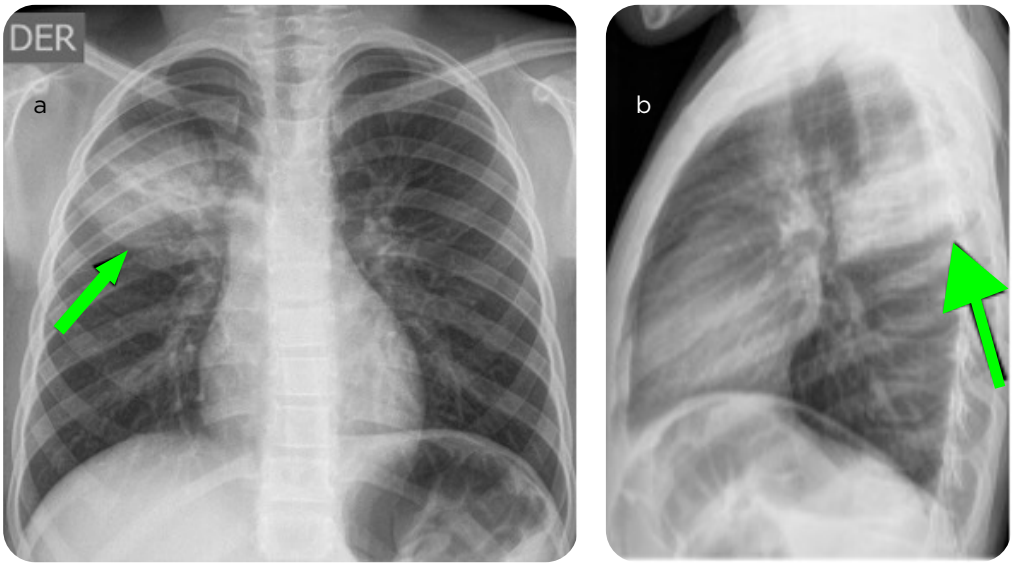


Figure 5. a and b) Chest X-ray, PA and lateral views. A 3-year-old patient with a round parenchymal opacity in the posterior segment of the right upper lobe (arrows); pneumococcal bacteremia was confirmed by blood culture.

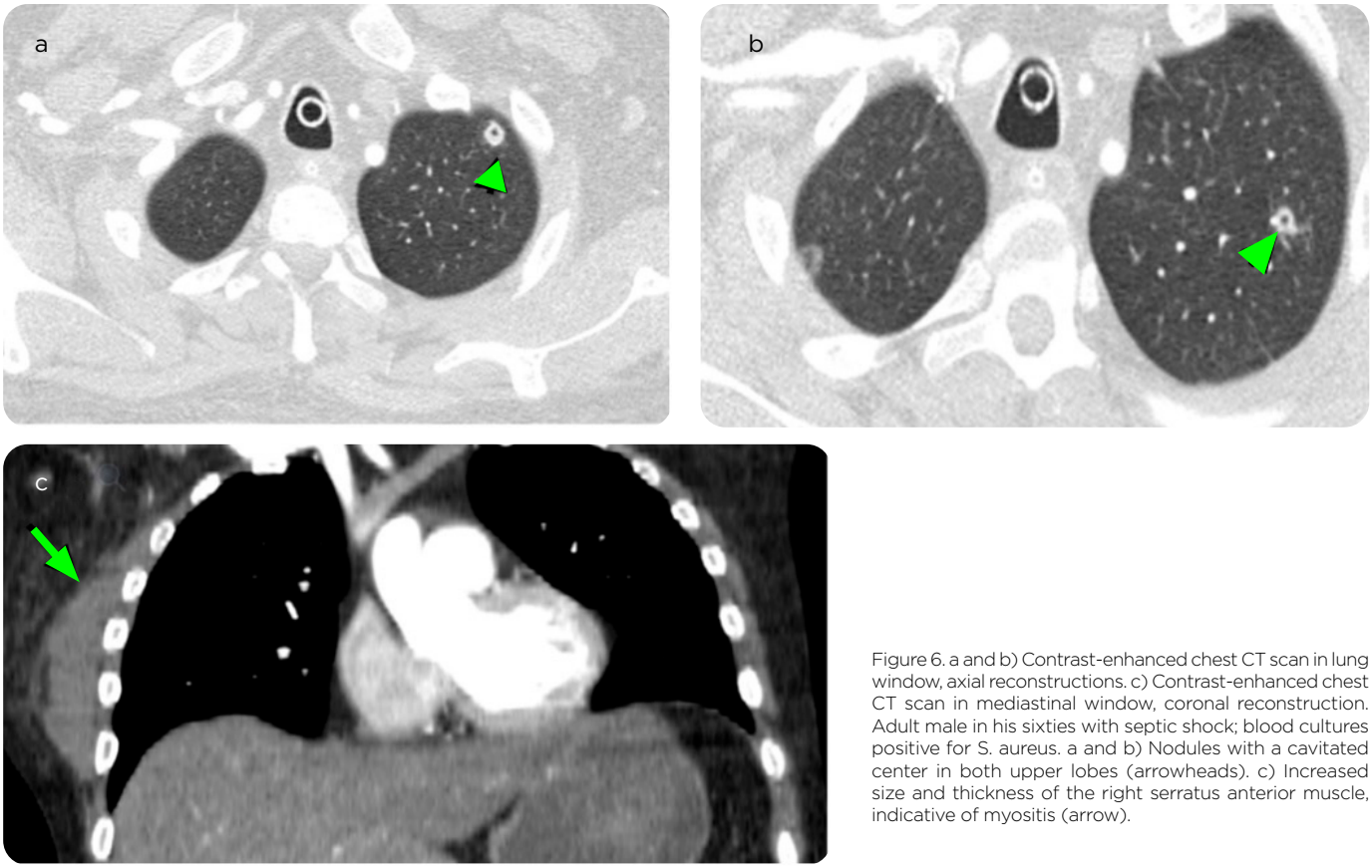


Figure 6. a and b) Contrast-enhanced chest CT scan in lung window, axial reconstructions. c) Contrast-enhanced chest CT scan in mediastinal window, coronal reconstruction. Adult male in his sixties with septic shock; blood cultures positive for S. aureus. a and b) Nodules with a cavitated center in both upper lobes (arrowheads). c) Increased size and thickness of the right serratus anterior muscle, indicative of myositis (arrow).

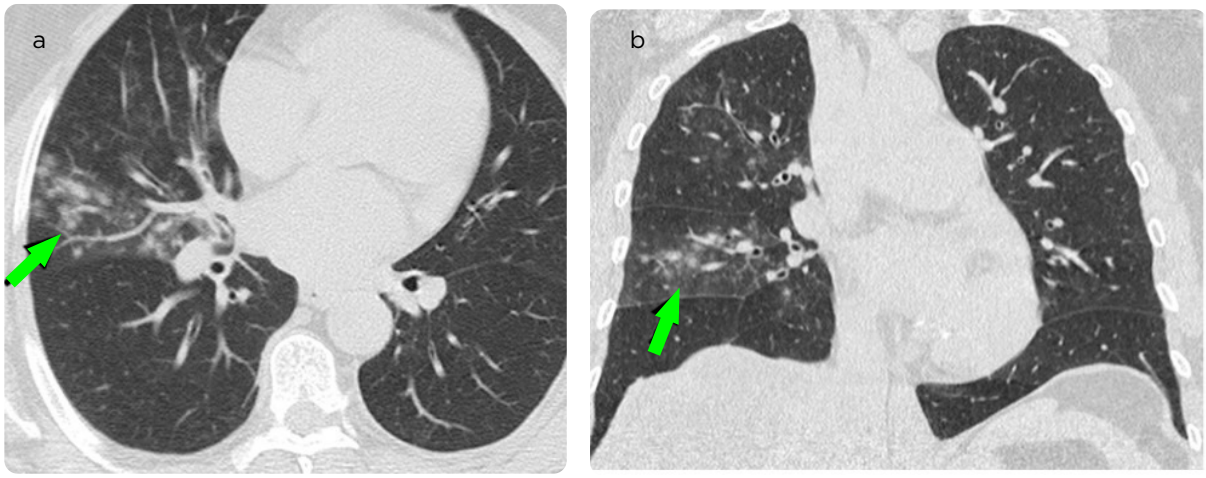


Figure 7. a and b) Chest CT scan with lung window, axial and coronal reconstructions. Centrilobular nodules in the middle lobe (arrows) with thickening of the bronchial walls.

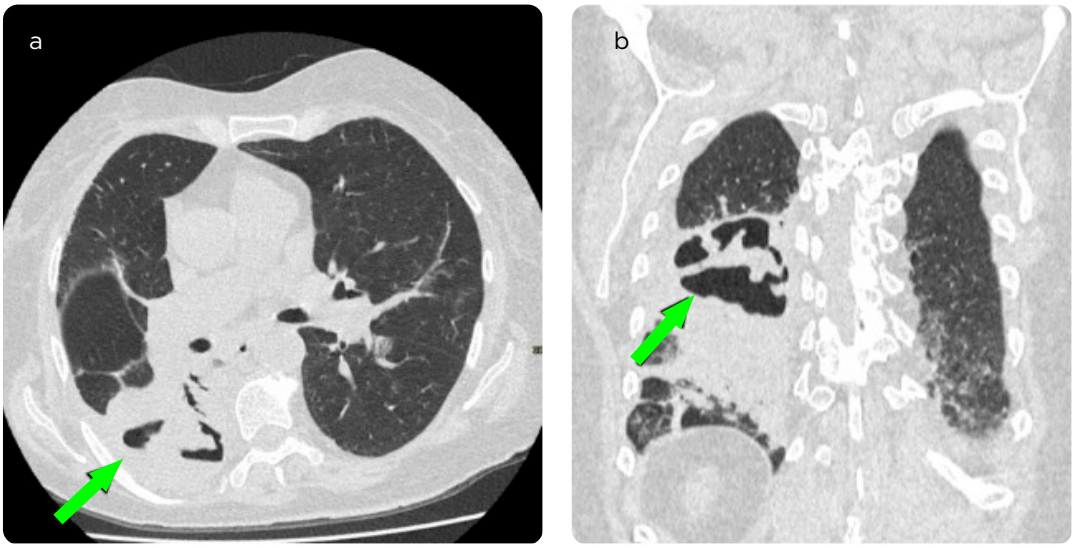


Figure 8. a and b) Chest CT scan with lung window and axial and coronal reconstructions. Consolidation with signs of volume loss in the posterior segment of the right upper lobe, as well as in the superior, posterior, and lateral segments of the right lower lobe, with associated cavitation and a fluid-air level in the posterior segment of the right upper lobe.

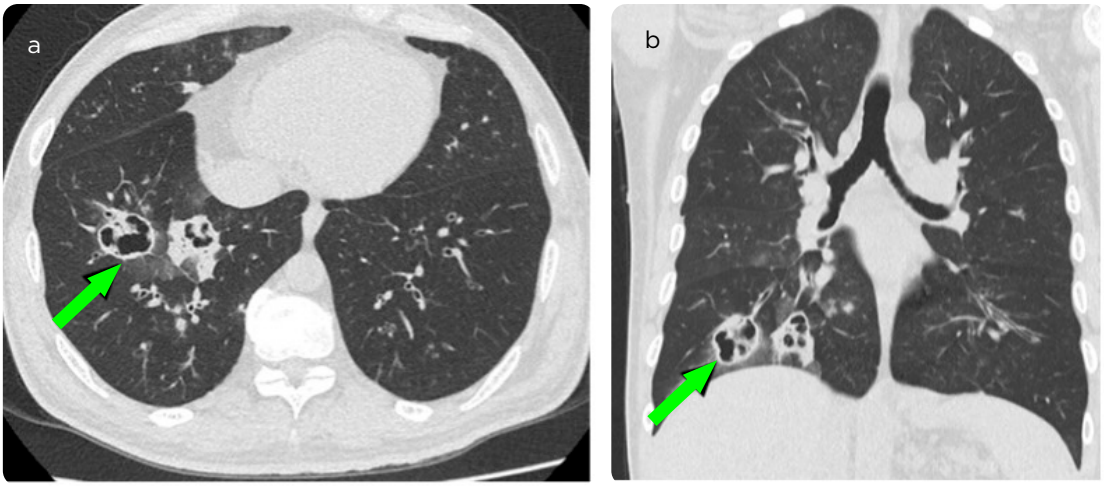


Figure 9. a and b) Contrast-enhanced chest CT, lung window, axial and coronal reconstructions. Thick-walled cavities in the right lower lobe (arrows), with adjacent "ground-glass" opacities.

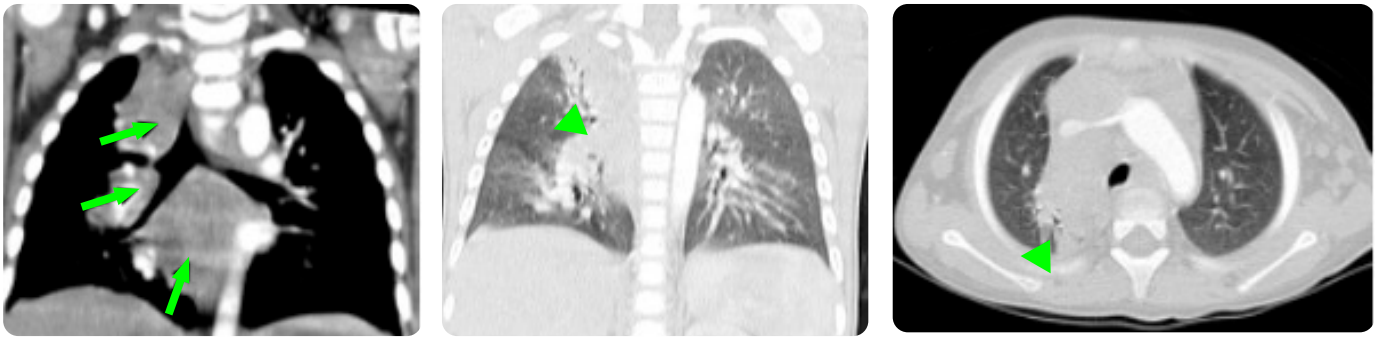


Figure 10. a) Contrast-enhanced chest CT, mediastinal window, coronal reconstruction. b and c) Contrast-enhanced chest CT, lung window, coronal and axial reconstructions. Pediatric patient diagnosed with tuberculosis. a) Adenopathy and mediastinal lymph node clusters (arrows), some with a hypodense center. b and c) Consolidation of the apical and posterior segments of the right upper lobe (arrowheads).

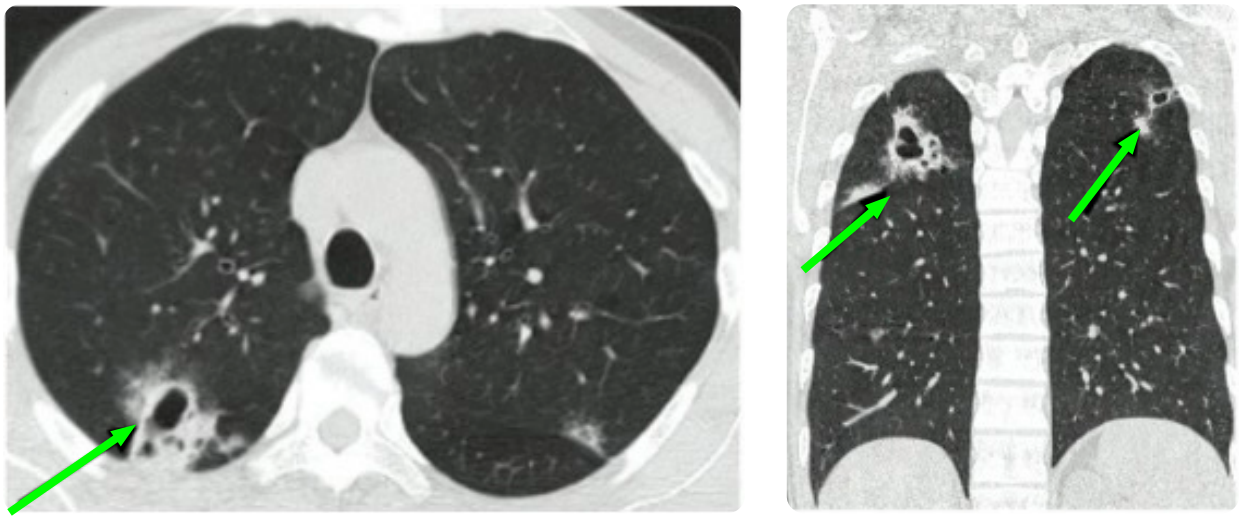


Figure 11. a and b) Chest CT in lung window with axial and coronal reconstructions. A 78-year-old patient with constitutional syndrome under investigation and chronic cough, PCR positive for TB. Cavities of varying sizes with thick, irregular walls involving both upper lobes (arrows).

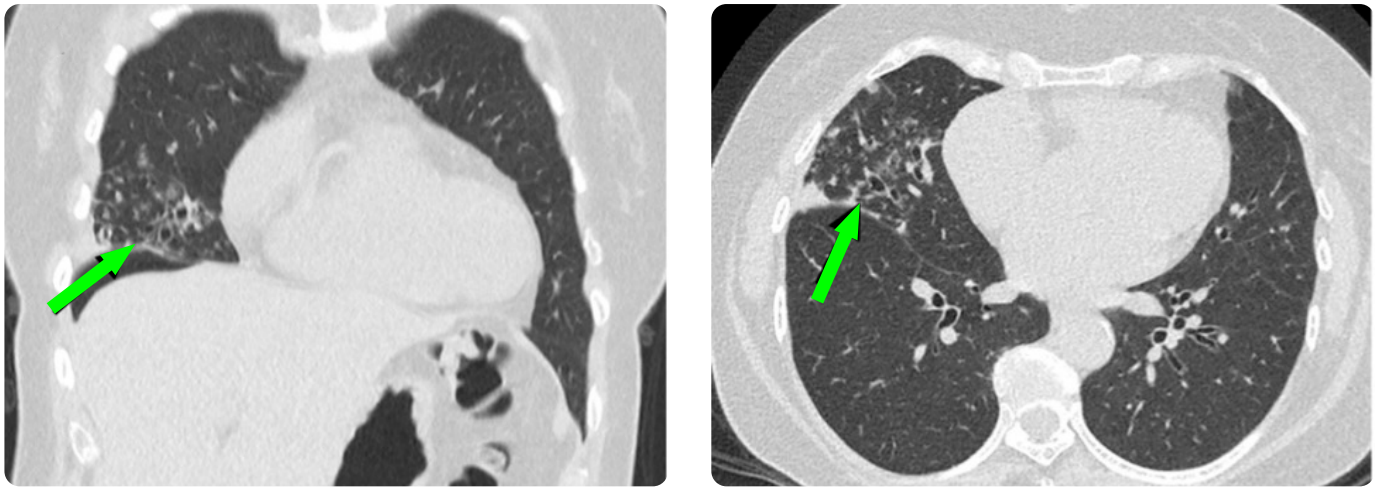


Figure 12. a and b) Chest CT in lung window in coronal and axial reconstructions. 60-year-old female patient. Centrilobular nodules in the middle lobe with bronchiectasis and volume loss (arrows).

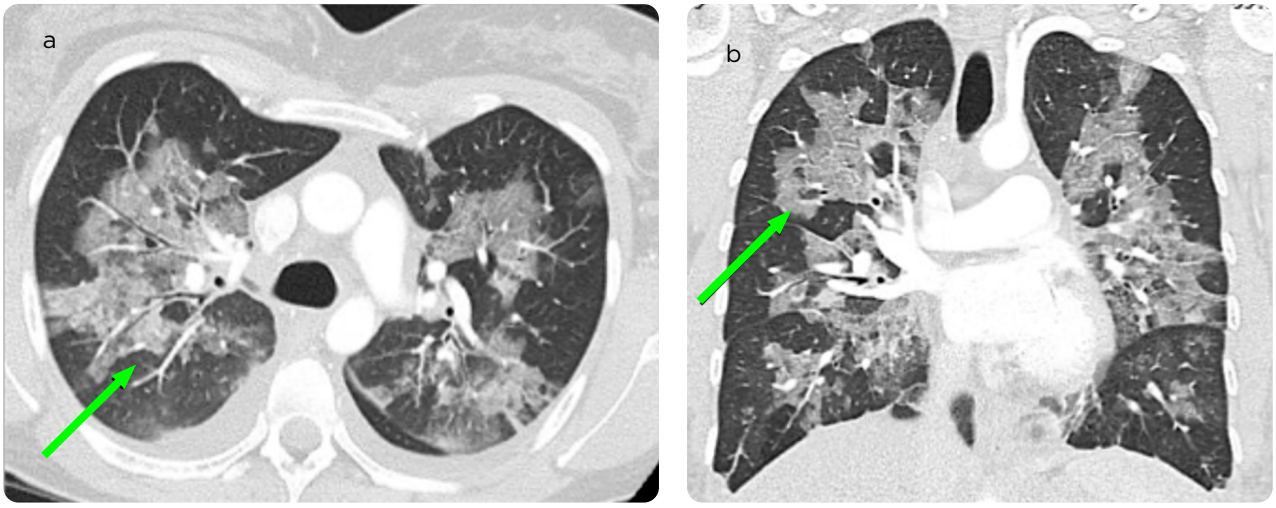


Figure 13. a and b) Chest CT scan with lung window settings in axial and coronal reconstructions. "Ground-glass" opacities with thickening of the interlobular septa, forming a "paving stone" pattern (arrows), predominantly in the central and peribronchovascular regions.

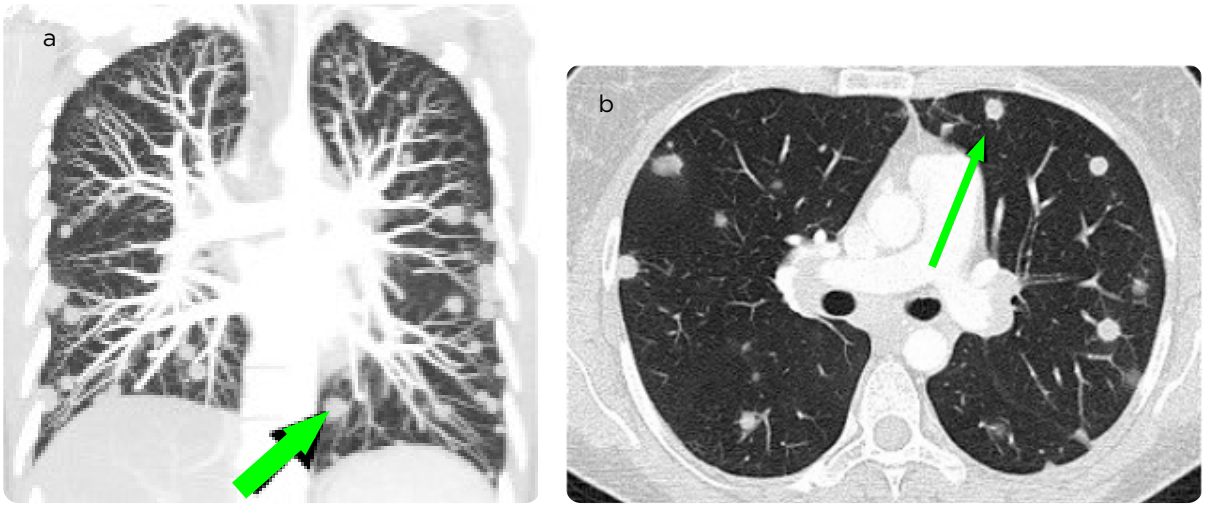


Figure 14. a and b) Chest CT scan with lung window settings in coronal (MIP) and axial reconstructions. Histoplasmomas appear as single or multiple soft-tissue density nodules (arrows) of varying sizes, randomly distributed in both lungs; due to their fibrous capsule, they generally have smooth margins.

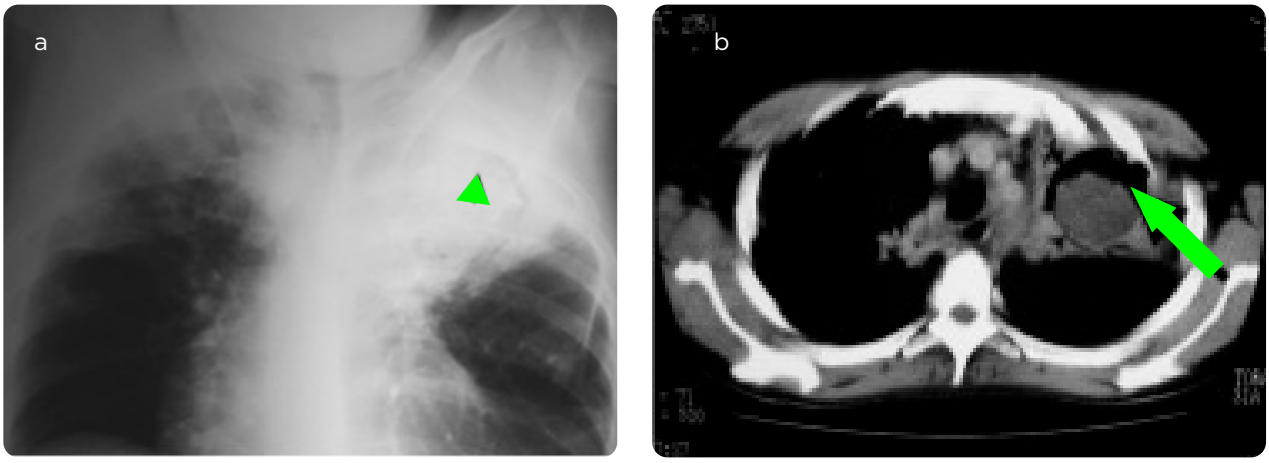


Figure 15. a) PA chest X-ray. b) Axial mediastinal-weighted chest CT scan. a) Consolidation in the left upper lobe with a semilunar-shaped radiolucency at its upper margin (arrowhead). b) Cavitation with a rounded lesion inside it, with soft-tissue density and air surrounding it, forming the "growing air" sign (arrow).

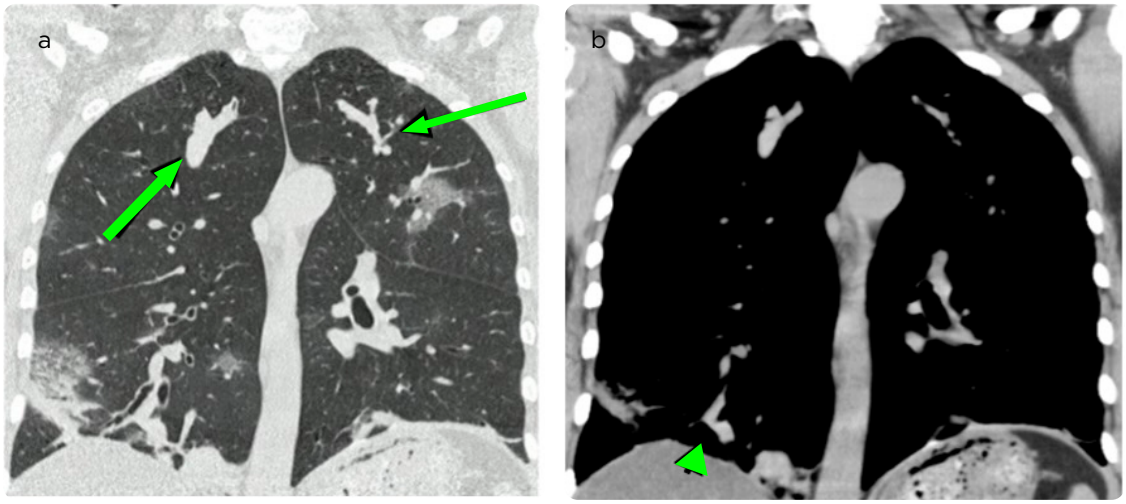


Figure 16. a and b) Chest CT scans in coronal sections using lung and mediastinal window settings; coronal reconstructions. A 51-year-old female patient with a history of asthma, presenting with dyspnea and cough. a) Bronchiectasis of segmental and subsegmental bronchi obstructed by secretions, predominantly in the upper lobes (arrows); central and peripheral "ground-glass" opacities. b) The material in the bronchi is hyperdense (arrowhead).

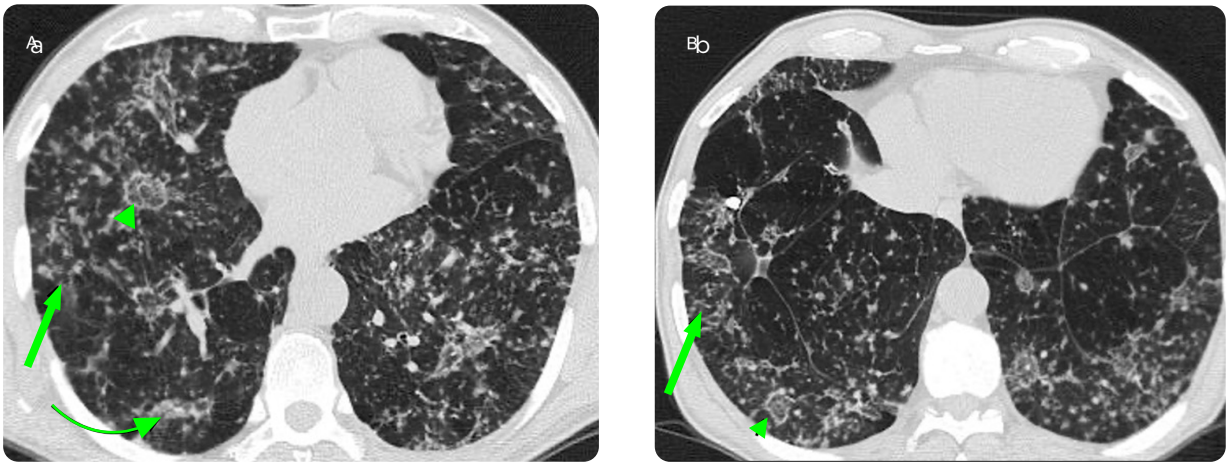


Figure 17. a and b) Chest CT in lung window on axial slices. Diffuse centrilobular nodules with a "budding tree" pattern (arrow) and "ground-glass" opacities (curved arrow) with surrounding consolidations forming a "reverse halo" pattern (arrowheads) in the visualized portion of the lower lobes, also with areas of architectural loss and fibrotic changes.

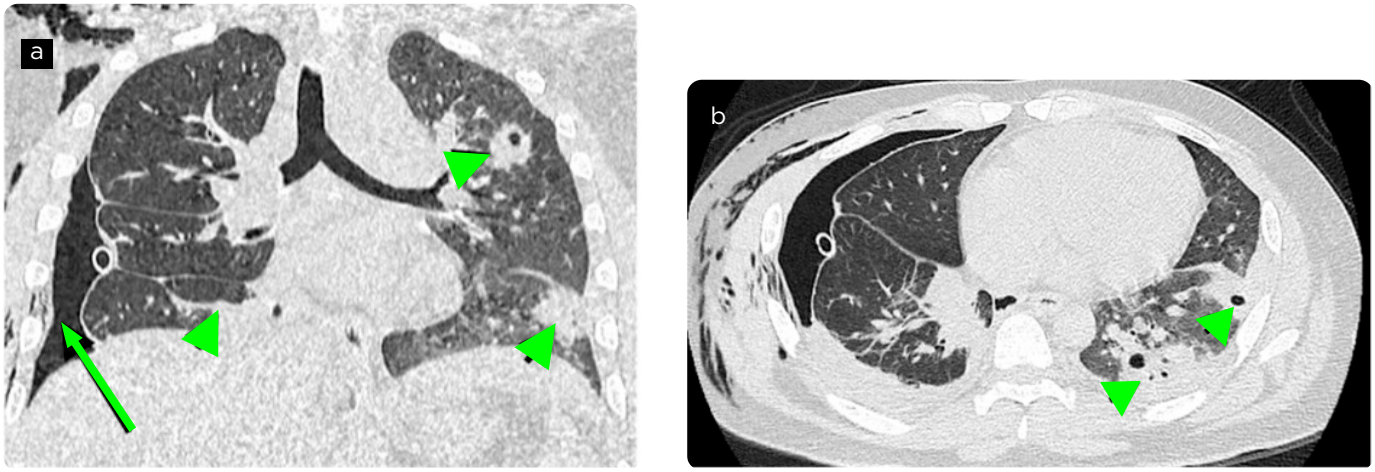


Figure 18. a and b) Chest CT scan in lung window, coronal and axial reconstructions. Right pneumothorax (arrow) with a thoracostomy tube and subcutaneous emphysema; in the parenchyma, some areas of consolidation are observed, predominantly subpleural and in the lower lobes (arrowheads), with a cavitated center.

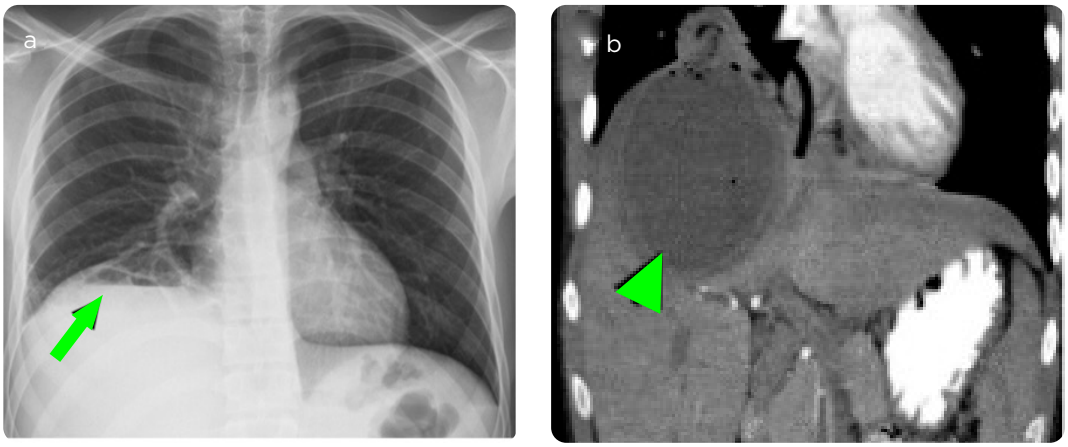


Figure 19. a and b) PA chest X-ray and abdominal CT scan in soft-tissue window, coronal reconstruction. a) Elevation of the right hemidiaphragm with a fluid-air level in the right lower lobe (arrow), with loss of diaphragmatic continuity. b) Image consistent with a hepatic abscess in segment VIII (arrowhead), extending by contiguity to the right lower lobe and the pleura, causing consolidation with gas bubbles within it (curved arrow).

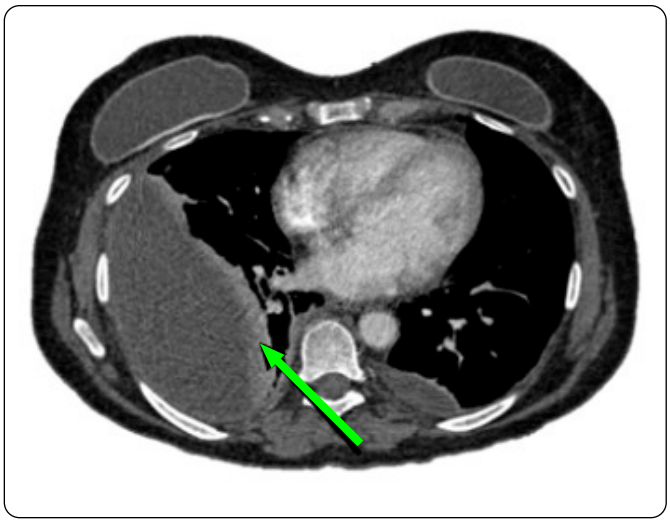


Figure 20. Axial mediastinal-window CT scan. Non-free-fluid-appearing right pleural effusion, with thickening of the pleural layers and enhancement (arrow), consistent with empyema.

• Viral agents

They are more common in young children, and the most common viral infections are those caused by respiratory syncytial virus (RSV), parainfluenza, and adenovirus (30). In adults, the most common are influenza A and B (6). The upper respiratory tract is usually affected during the initial phase (6). It causes tracheobronchitis, bronchiolitis, and pneumonia as it spreads to the small airways and alveoli (31). The epithelial lining of the respiratory tract is the primary target, and the bronchial and bronchiolar walls and the interstitium thicken due to edema. As inflammation increases, the alveoli fill with inflammatory exudate. Findings are typically nonspecific regarding the causative pathogen (32). They manifest as predominantly bilateral and diffuse reticular opacities, poorly defined nodules in the airspace, irregular areas of peribronchial "ground-glass" opacity, and consolidations (7). Hyperinflation may occur when the small airways are involved. They are rarely associated with complications or pleural effusion.

- **SARS-CoV2:** is an infectious disease caused by the severe acute respiratory syndrome coronavirus 2 (SARS-CoV-2) (33, 34). The first human cases of COVID-19 were reported in Wuhan, China, in December 2019 (33, 35). The World Health Organization (WHO) declared it a pandemic on March 11, 2020 (33, 36). Radiological findings are classified as typical, indeterminate, atypical, and negative for pneumonia (33). The typical appearance (with the highest specificity) includes peripherally distributed "ground-glass" opacities (Figure 1b), which are bilateral or multifocal, round in shape, with or without consolidation or visible intralobular lines ("cobblestone" pattern). The "inverted halo" sign or other findings of organized pneumonia may also be observed.
- **Respiratory syncytial virus (RSV):** The main risk factors are prematurity, heart disease, congenital abnormalities, and immunosuppression (3). Imaging may reveal "ground-glass opacities" (Figure 4), segmental consolidations, bronchial wall thickening, and centrilobular nodules. The involvement is bilateral and asymmetric, with a distribution that is more central than peripheral (37).
- **Influenza:** Influenza viruses are RNA viruses that cause seasonal respiratory infections (37). They manifest as "ground-glass" opacities, smooth thickening of the septa, centrilobular nodules, and patchy consolidations (less common), with a predominantly central distribution (Figure 13). It may be bilateral or unilateral and resemble heart failure without other findings such as cardiomegaly or pleural effusion (7).
- **Distinctive features:** The findings of viral pneumonias are very similar and overlap with one another. Some findings are more common in certain viruses than in others, such as multifocal involvement with consolidations and "ground-glass opacities" in adenovirus, and centrilobular nodules and pleural effusion in RSV (37) (Table 1). Parainfluenza, adenovirus, RSV, and influenza do not show marked extrapulmonary involvement.

Table 1. CT Findings of the Most Common Viral Pneumonias

Common Name	Distribution	Consolidation (%)	Ground-glass (%)	Nodules (%)	Thickening of bronchial walls	Pleural effusion
Adenovirus	Multifocal	50-75	50-75	Centrilobular 10-25	Infrequent	Common
Parainfluenza	Airway, multifocal	10-25	10-25	Centrilobular 25-50	Common	Infrequent
RSV	Airway, multifocal	10-25	10-25	Centrilobular 50- 75	Common	Common
Influenza	Airway, multifocal	10-25	10-25	25-50	Common	Infrequent

Source: adapted from Koo et al. (37).

Fungal agents

- **Histoplasmosis:** Histoplasma capsulatum is found in the soil of many temperate regions (7). Many cases occur after cleaning chicken coops or exploring caves infested with bats. It is common in the central and eastern United States, as well as in Central and South America (7, 38). It is caused by inhalation of spores, which tend to migrate to the mediastinal or hilar lymph nodes. In individuals with a competent immune system, the fungus multiplies intracellularly and cell-mediated immunity develops, causing intense inflammation and caseous necrosis that subsequently calcifies (7). In infants and patients with impaired T-cell-mediated immunity, progressive dissemination occurs (39). Most cases of symptomatic histoplasmosis occur in patients with a structural lung defect or an immunodeficiency, or when the infectious load is very high (7). There are two main groups of manifestations (5):

    - Acute symptomatic infection, which appears radiologically as patches of consolidation forming a bronchopneumonic pattern, mediastinal or hilar lymphadenopathy that may contain calcifications, or as one or multiple histoplasmomas (5, 7, 39, 40). Histoplasmomas appear as spherical nodules (ranging from a few millimeters to 4 cm) with soft-tissue density and random distribution (5) (Figure 14), with central calcification at three months (7).
    - Chronic infection occurs in structurally damaged lungs (emphysema), with invasion of cavities. Its radiological findings are similar to those of post-primary tuberculosis, such as multiple, small, patchy consolidations with cavitations, predominantly in the upper and bilateral lobes (7, 41). Pleural effusion and lymphadenopathy are uncommon.

- **Aspergilosis:** It is a fungal disease commonly caused by A. fumigatus, which grows in soil, water, decaying vegetation, and animal waste (7); it can present in different ways depending on the patient's immune status (3). It has been classified into saprophytic, allergic, and invasive forms, the latter occurring primarily in immunocompromised patients (3, 42, 43).

  An aspergilloma is a ball of mycelial hyphae that typically colonizes preexisting cavities without invading the parenchyma (5, 44). Imaging reveals round lesions within a thin-walled cavity or cyst, sometimes with a sign known as the "air crescent," which consists of a curved gas space surrounding the fungal ball within the cavity (5, 44). On CT, the fungal ball appears as a mass with air spaces that moves when the patient changes position (45) (Figure 15).

  Allergic bronchopulmonary aspergillosis (ABPA) is associated with asthma, elevated IgE levels, positive skin reactivity to Aspergillus, and positive serum precipitins (44). This is a hypersensitivity reaction to fungi, which causes their proliferation within the airway lumen, as well as bronchial dilation and trapping of large masses of mucus and Aspergillus hyphae, leading to mucoid impaction due to secretions (3, 5, 44). The images show central branching opacities, known as the "glove-finger pattern," which is also associated with air trapping, lobar consolidation, central bronchiectasis, and mucus-impacted bronchi, primarily in the upper lobes (5, 44). Mucus in the bronchi may appear hyperdense, likely due to calcium deposits (44, 46) (Figure 16).

- **Paracoccidiomicosis:** It is the most common systemic mycosis in Latin America (47). It is transmitted through inhalation of particles that cause parenchymal lung infection (48, 49). There are two forms: an acute form, which accounts for 5% of cases and primarily affects children and adolescents, and a chronic form, which accounts for 95% of cases and primarily affects men in their 30s. The latter results from the reactivation of quiescent pulmonary lesions (47). The acute form manifests primarily with mediastinal lymphadenopathy and pleural effusion (47, 50, 51). In the chronic form, the most common findings are "ground-glass" opacities, consolidations, nodules of varying sizes, masses, cavitations, interlobular septal thickening, and fibrotic lesions (47, 48, 52) (Figure 17). The distribution is usually bilateral and symmetrical, with predominant involvement of the peripheral and posterior regions. Extrapulmonary abnormalities may also occur (47).

Parasitic agents

- **Paragonimiasis:** It is caused by infection with Paragonimus westermani, an endemic disease in South America resulting from the consumption of undercooked seafood. Immature flukes penetrate the intestinal wall, travel through the peritoneal cavity, migrate through the diaphragm and pleura to enter the parenchyma (7). The images show multiple areas of consolidation with a rounded morphology and irregular borders, located primarily in the middle zone (53–55). Subpleural nodules with a necrotic center that may become cavitated can be observed, as well as thickening of the adjacent pleura and, occasionally, the worm's trail (Figure 18). Pleural effusion, pneumothorax, and hydropneumothorax may occur, and these are usually bilateral (7).
- **Amoebiasis:** Pleuropulmonary disease is the most common extraintestinal manifestation after liver abscess (56). The abscess may spread and involve the pleura and lung. Imaging findings include elevation of the right hemidiaphragm, pleural effusion or empyema, abscess or consolidation of the lower lobe, and hepatomegaly (Figure 19).

Complications

Pneumonia can lead to several complications. These include parapneumonic effusion, lung abscess, necrotizing pneumonia, and pneumothorax. Each is described below.

- **Parapneumonic effusion and empyema:** This refers to an accumulation of pus in the pleural space, which is a complication of pneumonia that occurs when the lung infection spreads to the pleura (8). The course of the condition can be divided into three stages (7, 8). Ultrasound helps confirm the effusion and ensure proper drainage. Echogenic pleural effusions, whether heterogeneous, septated or non-septated, or homogeneous, are always exudates, whereas hypoechoic effusions may be transudates or exudates (8). Most parapneumonic effusions and empyemas are septated (57). The appearance on CT depends on the pathophysiological stage. In the exudative phase, there is pleural fluid without significant pleural thickening (58). In the fibropurulent phase, the visceral and parietal pleuras typically appear thickened and separated by fluid, with the "split pleura" sign (59) and also with pleural enhancement (Figure 20). In the third phase, pulmonary fibrosis occurs with pulmonary entrapment due to the fibrotic reaction and extensive thickening.
- **Pulmonary abscess:** It may be secondary to pneumonia or obstruction by a foreign body (8). It corresponds to an area of parenchymal destruction with the formation of a suppurative collection within it. The images show a cavity with thick, irregular walls, a spherical morphology, and adjacent lung destruction or surrounding consolidation with an air-bronchogram extending throughout the area, with little or no compressive effect on the adjacent parenchyma (7, 8). It differs from empyema in that the abscess forms an acute angle with the chest wall, has a spherical shape (in all evaluated planes), a non-uniform thickened wall, and air-fluid levels (7, 60) (Figure 21).

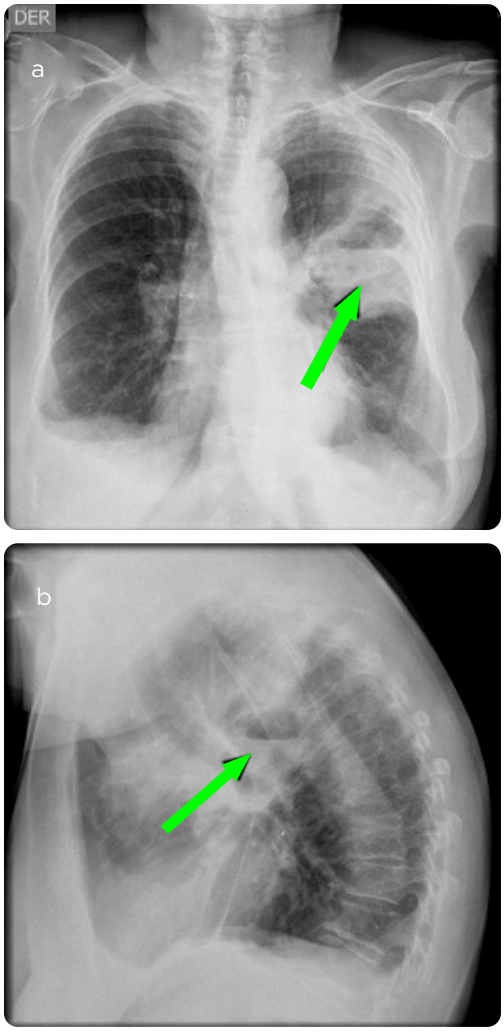


Figure 21. (a) and (b) Chest X-rays: PA and lateral views. A rounded opacity in the left upper lobe (arrows) with irregular borders that maintains its round shape across different planes, unlike empyema, in which the opacity may appear rounded in some planes but takes on a lenticular shape in others.

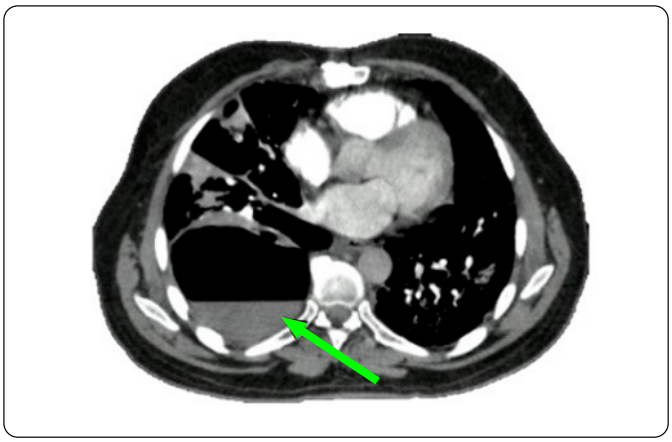


Figure 22. Contrast-enhanced chest CT scan in mediastinal window on an axial slice. Pediatric patient with community-acquired pneumonia. A thin-walled, round cystic lesion in the lung parenchyma of the right lower lobe (arrow), adjacent to the bronchial tree, with an air-fluid level within it.

- **Necrotizing pneumonia:** This corresponds to necrotic tissue in an infected lung, caused primarily by Staphylococcus aureus infection (5). Arteritis and vascular thrombosis can lead to ischemic necrosis and the death of a portion of the lung. It appears on images as hypodense areas within a consolidated lobe or segment, associated with multiple cavitations (Figure 8), often with air-fluid levels. A cavitation is an abnormal structure filled with gas or fluid, typically with a thick, irregular wall, resulting from the expulsion or drainage of a necrotic portion of the lesion through the bronchial tree (61).
- **Pneumocele:** A thin-walled gas-filled space in the lung, caused by pneumonia or trauma (61). It results from a combination of parenchymal necrosis and airway obstruction due to a valve mechanism that prevents air from escaping, thereby promoting dilation and the formation of the pneumothorax. It appears as a round, thin-walled air space, usually surrounded by lung parenchyma and containing a small amount of fluid (62) (Figure 22). It may predispose to spontaneous pneumothorax.

Conclusions

Lung infections are one of the leading causes of morbidity and mortality worldwide. A thorough understanding of their pathophysiology is essential for recognizing the characteristic radiological patterns associated with each causative agent, which facilitates the identification of the responsible pathogen and, consequently, enables more precise and effective treatment.

Bacterial infections are the most common and typically present as lobar pneumonia or bronchopneumonia, depending on the distribution of the inflammatory process. In contrast, viral infections tend to present with a pattern of interstitial pneumonia, in which radiological images are often similar across different viral agents, which can make precise identification difficult without the use of other diagnostic methods.

On the other hand, fungal infections are characterized by the formation of pulmonary nodules that often progress to cavitation. Parasites, depending on their route of dissemination, can cause a variety of pulmonary manifestations ranging from diffuse infiltrates to localized lesions, which also influences the radiological pattern observed.

Finally, early identification of pulmonary complications such as abscesses, pleural effusions, or pneumothorax is essential to provide timely treatment to patients, thereby reducing morbidity and improving clinical outcomes.

References

1. Martínez-Vernaza S, McKinley E, Soto MJ, Gualtero S. Neumonía adquirida en la comunidad: una revisión narrativa. Univ Med. 2018;59(4):1-10. http://dx.doi.org/10.11144/Javeriana.umed59-4.neum.
2. Jain V, Vashisht R, Yilmaz G, et al. Pneumonia pathology. [Updated 2023 Jul 31]. En: StatPearls [Internet]. Treasure Island (FL): StatPearls Publishing; 2023 Jan. https://www.ncbi.nlm.nih.gov/books/NBK526116/
3. Franquet T, Chung JH. Imaging of pulmonary infection. En: Hodler J, Kubik-Huch R, von Schulthess G, editors. Diseases of the chest, breast, heart and vessels 2019-2022. IDKD Springer Series. Springer, Cham; 2019. https://doi.org/10.1007/978-3-030-11149-6_7.
4. Jokerst C. Acute respiratory illness in immunocompetent patients. American College of Radiology. 2024. https://acsearch.acr.org/docs/69446/Narrative/.
5. McLoud TC, Boiselle PM. Pulmonary infections in the normal host. Thoracic Radiology. 2010:80-120. https://doi.org/10.1016/B978-0-323-02790-8.00003-2.
6. Garg M, Prabhakar N, Gulati A, Agarwal R, Dhooria S. Spectrum of imaging findings in pulmonary infections. Part 1: Bacterial and viral. Pol J Radiol. 2019;84:e205-e213. https://doi.org/10.5114/pjr.2019.85812.
7. Infections of the lung and pleura. Webb WR, Higgins CB, editors. Imaging diseases of the chest. 5th ed. Philadelphia: Elsevier Saunders; 2017. p. 351–416.
8. Reynolds JH, McDonald G, Alton H, Gordon SB. Pneumonia in the immunocompetent patient. Br J Radiol. 2010;83:998-1009. https://doi.org/10.1259/bjr/31200593.
9. Felson L, Rosenberg L, Hamburger M. Roentgen findings in acute Friedlander's pneumonia. Radiology. 1949;53:559-65.
10. Holmes R. Friedlander's pneumonia. AJR Am J Roentgenol. 1956;75:728-47.
11. Groskin SA, Panicek DM, Ewing DK, et al. Bacterial lung abscess: a review of the radiographic and clinical features of 50 cases. J Thorac Imaging. 1991;6:62-7.
12. Bartlett JG, Finegold SM. Anaerobic infections of the lung and pleural space. Am Rev Respir Dis. 1974;110:56-77.
13. Levison ME. Anaerobic pleuropulmonary infection. Curr Opin Infect Dis. 2001;14:187-91.
14. Mojon P. Oral health and respiratory infection. J Can Dent Assoc. 2002;68:340-5.
15. Franquet T. Imaging of pneumonia: trends and algorithms. Eur Respir J. 2001;18:196-208.
16. Landay MJ, Christensen EE, Bynum LJ, et al. Anaerobic pleural and pulmonary infections. AJR Am J Roentgenol. 1980;134:233-40.
17. Gupta R, Espinal MA, Raviglione MC. Tuberculosis as a major global health problem in the 21st century: a WHO perspective. Semin Respir Crit Care Med. 2004;25:245-53.
18. Dye C, Scheele S, Dolin P, et al. Consensus statement. Global burden of tuberculosis: estimated incidence, prevalence, and mortality by country. WHO Global Surveillance and Monitoring Project. JAMA. 1999;282:677-86.
19. Woodring JH, Vandiviere HM, Fried AM, et al. Update: the radiographic features of pulmonary tuberculosis. AJR Am J Roentgenol. 1986;146:497–506.
20. Baran R, Tor M, Tahaoglu K, et al. Intrathoracic tuberculous adenopathy: clinical and bronchoscopic features in 17 adults without parenchymal lesions. Chest. 1996;51:87-9.
21. Berger HW, Granada MG. Lower lung field tuberculosis. Chest. 1974;65:522-6.
22. Im JG, Itoh H, Han MC. CT of pulmonary tuberculosis. Semin Ultrasound CT MR. 1995;16(5):420-34.
23. Rossi SE, Franquet T, Volpacchio M, Gimenez A, Aguilar G. Tree-in-bud pattern at thin-section CT of the lungs: radiologic-pathologic overview. Radiographics. 2005;25(3):789-801.
24. Kendall BA, Winthrop KL. Update on the epidemiology of pulmonary nontuberculous mycobacterial infections. Semin Respir Crit Care Med. 2013;34(1):87-94.
25. Falkinham JO III. Nontuberculous mycobacteria in the environment. Clin Chest Med. 2002;23:529-51.
26. Glassroth J. Pulmonary disease due to nontuberculous mycobacteria. Chest. 2008;133:243-51.
27. Ellis SM, Hansell DM. Imaging of non-tuberculous (atypical) mycobacterial pulmonary infection. Clin Radiol. 2002;57:661-9.
28. Contreras MA, Cheung OT, Sanders DE, et al. Pulmonary infection with nontuberculous mycobacteria. Am Rev Respir Dis. 1988;137:149-52.
29. O'Brien RJ. The epidemiology of nontuberculous mycobacterial disease. Clin Chest Med. 1989;10:407-18.
30. Daltro P, Santos EN, Gasparetto TD, et al. Pulmonary infections. Pediatr Radiol. 2011;41(Suppl 1):S69-S82.
31. Beigelman-Aubry C, Godet C, Caumes E. Lung infections: the radiologist's perspective. Diagn Interv Imaging. 2012;93:431-40.
32. Kim EA, Lee KS, Primack SL, et al. Viral pneumonias in adults: radiologic and pathologic findings. RadioGraphics. 2002;22:S137-49.
33. Kwee TC, Kwee RM. Chest CT in COVID-19: What the radiologist needs to know. Radiographics. 2020;40(7):1848-65.
34. World Health Organization. Coronavirus. 2025. https://www.who.int/health topics/coronavirus#tab=tab_1.
35. World Health Organization. Pneumonia of unknown cause: China. 2025. https://www.who.int/csr/don/05-january-2020-pneumonia-of-unkown-cause-china/en/.
36. World Health Organization. WHO announces COVID-19 outbreak a pandemic. 2020. http://www.euro.who.int/en/health-topics/health-emergencies/coronavirus-covid-19/news/news/2020/3/who-announces-covid-19-outbreak-a-pan-demic.

37. Koo HJ, Lim S, Choe J, Choi SH, Sung H, Do KH. Radiographic and CT features of viral pneumonia. Radiographics. 2018;38(3):719-39.
38. Severo LC, Oliveira FM, Irion K, et al. Histoplasmosis in Rio Grande do Sul, Brazil: a 21-year experience. Rev Inst Med Trop Sao Paulo. 2001;43:183-7.
39. Johnson P, Sarosi G. Histoplasmosis. Semin Respir Med. 1987;9:145-51.
40. Gurney JW, Conces DJ. Pulmonary histoplasmosis. Radiology. 1996;199:297-306.
41. Baum G, Schwarz J. Chronic pulmonary histoplasmosis. Am J Med. 1962;33:873-9.
42. Franquet T, Muller NL, Giménez A, Guembe P, de La Torre J, Bague S. Spectrum of pulmonary aspergillosis: histologic, clinical, and radiologic findings. Radiographics. 2001;21(4):825-37.
43. Gefter WB. The spectrum of pulmonary aspergillosis. J Thorac Imaging. 1992;7(4):56-74.
44. Garg M, Prabhakar N, Gulati A, Agarwal R, Dhooria S. Spectrum of imaging findings in pulmonary infections. Part 2: Fungal, mycobacterial, and parasitic. Pol J Radiol. 2019;84:e214-e223.
45. Prasad A, Agarwal K, Deepak D, Atwal SS. Pulmonary aspergillosis: What CT can offer before it is too late! J Clin Diagn Res. 2016;10:TE01-TE05.
46. Franquet T, Müller NL, Oikonomou A, Flint JD. Aspergillus infection of the airways: computed tomography and pathologic findings. J Comput Assist Tomogr. 2004;28:10-6.
47. Barreto MM, et al. Thoracic paracoccidioidomycosis: Radiographic and CT findings. RadioGraphics. 2012;32(1):71-84.
48. Funari M, Kavakama J, Shikanai-Yasuda MA, et al. Chronic pulmonary paracoccidioidomycosis (South American blastomycosis): high-resolution CT findings in 41 patients. AJR Am J Roentgenol. 1999;173(1):59-64.
49. do Valle AC, Guimarães RR, Lopes DJ, Capone D. Thoracic radiologic aspects in paracoccidioidomycosis [en Portugues]. Rev Inst Med Trop Sao Paulo. 1992;34(2):107-15.
50. Ferreira MS. Paracoccidioidomycosis. Paediatr Respir Rev. 2009;10(4):161-5.
51. Benard G, Kavakama J, Mendes-Giannini MJ, Kono A, Duarte AJ, Shikanai-Yasuda MA. Contribution to the natural history of paracoccidioidomycosis: identification of the primary pulmonary infection in the severe acute form of the disease-a case report. Clin Infect Dis. 2005;40(1):e1-e4.
52. Souza AS Jr, Gasparetto EL, Davaus T, Escuissato DL, Marchiori E. High-resolution CT findings of 77 patients with untreated pulmonary paracoccidioidomycosis. AJR Am J Roentgenol. 2006;187(5):1248-52.
53. Johnson RJ, Johnson JR. Paragonimiasis in Indochinese refugees. Roentgenographic findings with clinical correlations. Am Rev Respir Dis. 1983;128:534-8.
54. Ogakwu M, Nwokolo C. Radiological findings in pulmonary paragonimiasis as seen in Nigeria: a review based on one hundred cases. Br J Radiol. 1973;46:699-705.
55. Taylor CR, Swett HA. Pulmonary paragonimiasis in Laotian refugees. Radiology. 1982;143:411-2.
56. Shamsuzzaman SM, Hashiguchi Y. Thoracic amebiasis. Clin Chest Med. 2002;23:479-92.
57. Evans A, Gleeson F. Radiology in pleural disease: state of the art. Respirology. 2004;9:300-12.
58. Janet E. Complex diseases of the pleural space: radiographic and CT interpretation. Radiographics. 1997;17:63-79.
59. Kraus G. The split pleura sign. Radiology. 2007;243:297-8.
60. Stark DD, Federle MP, Goodman PC, Podrasky AE, Webb WR. Differentiating lung abscess and empyema: radiography and computed tomography. AJR Am J Roentgenol. 1983;141(1):163-7.
61. Bankier AA, MacMahon H, Colby T, Gevenois PA, Goo JM, Leung ANC, Lynch DA, Schaefer-Prokop CM, Tomiyama N, Travis WD, Verschakelen JA, White CS, Naidich DP. Fleischner Society: glossary of terms for thoracic imaging. Radiology. 2024;310(2):e232558. https://doi.org/10.1148/radiol.232558.
62. Quigley MJ, Fraser RS. Pulmonary pneumatocele: pathology and pathogenesis. AJR Am J Roentgenol. 1988;150(6):1275-7.

Correspondence

José David Brito Araújo
Departamento de Imágenes Diagnósticas, Hospital Universitario San Ignacio
Carrera 9 # 96-08 Bogotá, Colombia
josebrito@javeriana.edu.co

Received for evaluation: July 10 20, 2024
Accepted for publication: September 30, 2024